Proc AICWEMC, Bangalore, India
18-26 Nov. 1985
pp. 79-82

Electromagnetics, Vol. 9, No. 1, 1989
pp. 69-84

Sensor and Simulation Notes
Note 284
22 May 1984

AIRBORNE PLATFORM FOR MEASUREMENT OF TRANSIENT OR BROADBAND CW ELECTROMAGNETIC FIELDS

by

D.V. Giri
LuTech, Inc.
3516 Breakwater Court, Hayward, CA 94545

and

Carl E. Baum
Air Force Weapons Laboratory
Kirtland AFB, NM 87117

Abstract

This note deals with the development of considerations and guidelines useful in designing an airborne platform for transient or broadband CW electromagnetic (EM) field measurement. The EM problem consists of choosing the appropriate sensor type and location such that scattered fields from the aircraft and the sensor mounting do not significantly couple to the sensor, while measuring the incident field. The EM considerations of such a sensor design are discussed in this note.

Contents

I. Introduction

In performing measurements of physical quantities, more often than not, the effect of the measuring device or instrumentation on the measurement can lead to inaccuracies. Estimation of such effects, combined with properly designed engineering compromises are imperative in making meaningful measurements. In the present example, the physical quantities are electromagnetic fields maintained in air by a radiating source, natural or man-made, and the measuring instrumentation is aboard an aircraft in flight. The object of this note is then to deal with the conceptual development of techniques for transient or broadband CW electromagnetic field measurement from an airborne platform, which was briefly introduced in [1] and addressed in detail here.

Past measurements of electromagnetic quantities from airborne platforms include antennas on aircraft and instrumented aircraft with surface mounted sensors [2]. For example, in investigating the natural lightning phenomenon, an instrumented aircraft [1] with $\dot{B}$ and $\dot{D}$ sensors [3,4] mounted on the aircraft skin has been used and a large amount of data gathered over the past several years.

In measurement configurations, such as above, conceptually one can think of locating an electric sensor at the null of the principal fuselage resonance. However, as past computations have shown [5,6], the natural modes associated with the fuselage resonances are complex and a perfect null does not exist. Even the use of a symmetric mode charge function minimum in the "middle" of fuselage for an electric field sensor location, has little practical significance, since such a scheme applies at best to one symmetric mode and many of the higher order symmetric modes will couple to the sensor. Such coupling will contaminate the measured signal corresponding to the incident field that is present in the absence of the aircraft.

Consider now that the scattered field from the aircraft has both symmetric and antisymmetric parts for the aircraft exterior with respect to a symmetry plane. Consequently, there is a choice of placing the sensor so that it responds to only one part (symmetric or antisymmetric) in such a way that the coupling from the other part (antisymmetric or symmetric) is minimized (ideally zero). In addition, the sensor type (electric or magnetic) is an important consideration. Several factors impact these choices, e.g., the sensor has to be physically away from the airframe to reduce its sensitivity to low frequency scattered fields. Once the sensor is physically removed and connected by cables and shields, the free end of the cable or shield (boom) becomes a charge maximum or current minimum calling for a magnetic rather than electric field sensor. Alternatively, if one is interested in electric field measurement, a platform dielectrically isolated from the airframe is desirable. Such an isolated platform could cause operation and instrumentation problems, where the measured signal would be brought into the aircraft for storage and processing via telemetry. The subject of electric field measurement from airborne platforms deserves much attention in future studies.

In concluding this introductory section, it is noted that several issues that govern airborne electromagnetic platforms have been identified and they will all be addressed in detail in the following sections.

II. Use of Symmetry in Measurements

As was pointed out earlier, both the incident and scattered fields from the aircraft have two parts viz., symmetric and antisymmetric. The two parts do not couple to each other and can be treated separately. It is assumed that the incident field is arbitrarily oriented so that it has both symmetric and antisymmetric parts, for measurement. They are illustrated in Figure 1 reproduced from [7]. It is observed that the symmetry plane P is a vertical plane passing through the fuselage with one wing on either side. In the symmetric part, the net fuselage current flows from tail to nose, while the wing currents flow outward from the fuselage to the wing tip, for the given incident field configuration. In the antisymmetric part, there is no net fuselage current while the wing (and/or the horizontal stabilizer) current flows from the wing tip to wing tip. The reason why such symmetry decomposition of fields and currents is useful for measurement can be explained as follows.

Consider the objective of locating an electric or magnetic field sensor on or near the aircraft for measuring the incident electric or magnetic field. The coupling of the incident field with the aircraft results in surface currents and charges which maintain the total field. The symmetry decomposition helps in thinking about the fields in terms of two mutually exclusive and complementary parts. For instance, if one were to measure an incident antisymmetric magnetic field, an excellent choice of location for a sensing loop is on the fuselage axis (aft or forward) so that its axis is aligned parallel to the incident magnetic field which is parallel to the fuselage (see Figure 1b). It is observed that such an orientation of the sensor is insensitive to magnetic field scattered by fuselage resonances and the sensor responses to magnetic fields of symmetric currents on transverse elements (wings and horizontal stabilizer) cancel out. Thus, such a sensor responds to antisymmetric incident magnetic field and magnetic field scattered by antisymmetric currents on transverse elements. The sensitivity to antisymmetric transverse currents can be minimized by considerations such as geometry and physical distances etc.

As a second example, consider the measurement of a symmetric component of

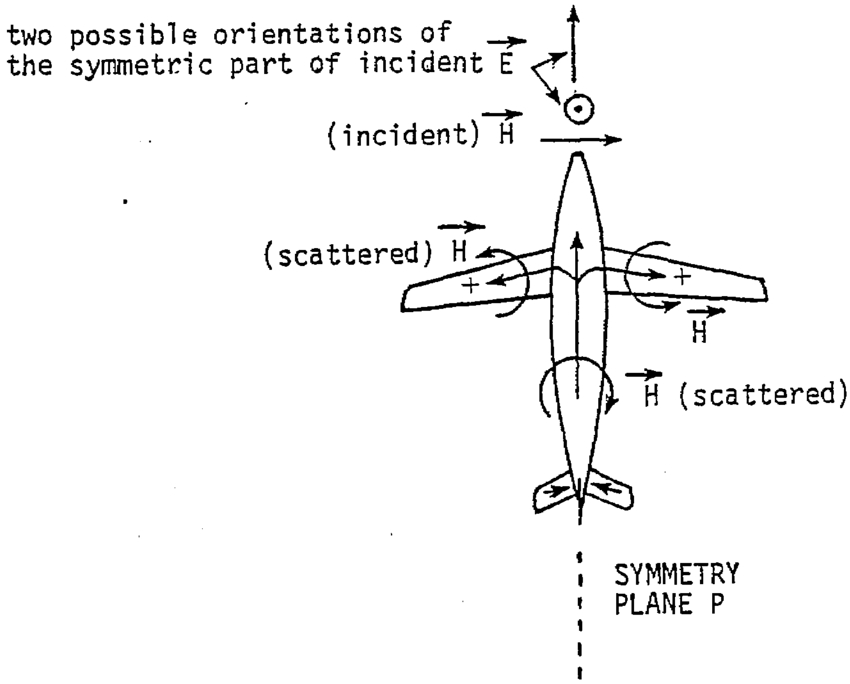

A. Symmetric Part: Top View

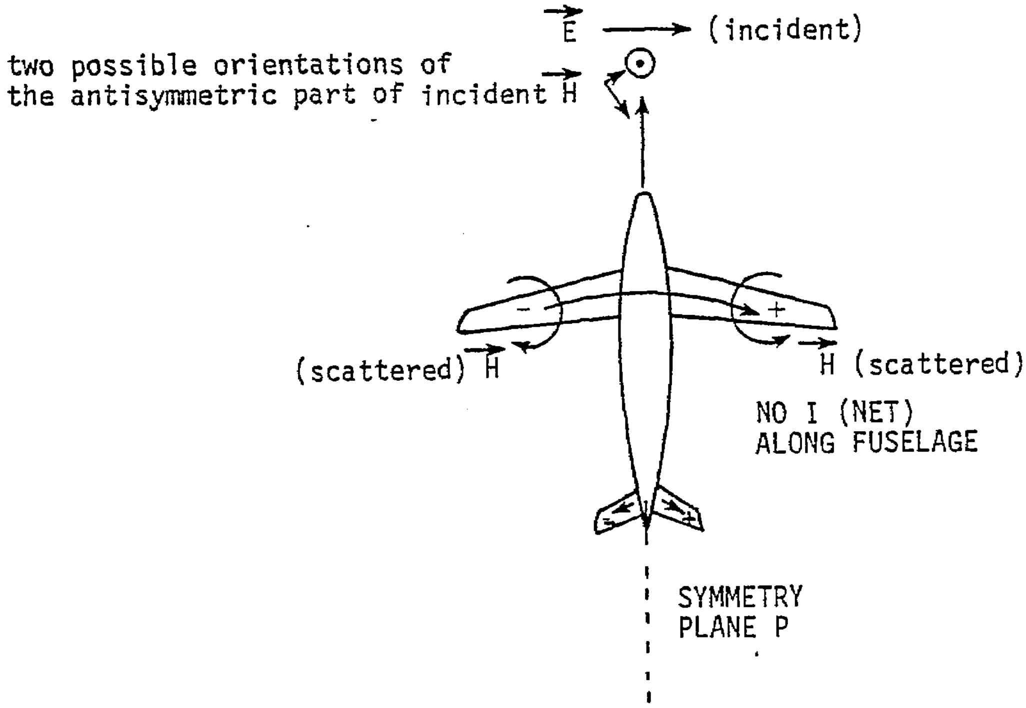

B. Antisymmetric Part: Top View

Figure 1. The symmetry plane of a generalized aircraft showing the symmetric and antisymmetric parts [7].

the incident magnetic field (see Figure 1a) with two sensing loops at or near wing tips with their axes parallel to the incident symmetric magnetic field. This orientation makes the sensors insensitive to antisymmetric scattered magnetic fields. By appropriately combining the two signals, the antisymmetric part is ideally exactly cancelled and only a symmetric part is left. The scattered fields due to symmetric currents on fuselage, wings, horizontal and vertical stabilizers can be minimized by appropriate placement and orientation near the wing tips. So at least in principle, such a measurement is possible, but would have to be considered in detail.

Next, one may consider measuring an incident antisymmetric magnetic field parallel to the fuselage in Figure 1b with two sensors at or near wing tips. Of course, the sensors will be oriented symmetrically with their axes nearly parallel to the fuselage to respond to the incident field. They will naturally be insensitive to fuselage currents. Symmetric wing and horizontal stabilizer currents induce opposing signals in the two sensors and the antisymmetric wing and horizontal stabilizer currents induce additive or in phase signals in the two sensors. By adding the two detected signals, the symmetric part of scattered field can be cancelled out and by subtracting the two detected signals, the antisymmetric part of scattered field can be cancelled out. However, one is still left with three unknowns (voltages corresponding to the incident antisymmetric magnetic field, and symmetric and antisymmetric scattered magnetic fields) and two known signals (voltages measured on the left and right wing tip sensors), making it difficult to measure the incident antisymmetric field. The antisymmetric scattered field response can be minimized by finding a null location near the wing tips and the antisymmetric incident field is measurable by addition of two sensor pickup voltages. Consequently, the incident antisymmetric magnetic field approximately parallel to the fuselage, is probably best measured by a single sensing loop on the fuselage axis aft or forward depending on the aircraft.

In concluding this section, it is emphasized that symmetry decomposition of incident and scattered fields is extremely useful in simplifying the understanding of electromagnetic interaction with an object like the aircraft which has an approximate symmetry plane. In addition, this note focuses attention on the measurement of magnetic fields which is easier on an airborne platform than the electric field measurement owing to instrumentation cabling considerations. Once the magnetic field is picked for measurement, it contains both symmetric and antisymmetric components, if the aircraft is arbitrarily oriented with respect to the incident field. The antisymmetric incident magnetic field approximately parallel to the fuselage, is best measured by a single sensor on or near the fuselage axis in the symmetry plane. The symmetric incident magnetic field can be measured by two sensors at wing tips and appropriately combining their signals.

III. Measurement of Fields by Sensors

The sensors used in airborne electromagnetic platforms convert the desired electromagnetic field parameter to voltage or current at a connector or terminal. If one does not use telemetry this implies that the sensors which are physically removed from the airframe to avoid low frequency scattered signals, have to be connected by cables and/or shields to the instrumentation inside the aircraft. Therefore the topology of sensor mounts, cables, and shields become important in designing experiments [4]. In addition symmetry considerations of sensors could also be important in some cases. In this section, the topological and symmetry considerations of the sensors along with their associated mountings and connecting cables are outlined.

A. Topological Considerations

Consider for instance, a sensor near the airframe as a fundamental component of an electromagnetic measurement. The signal sensed must be transported to the recording instrumentation inside the aircraft via cables (typically well shielded coaxial or twin-axial cables) without disturbing the quantities of interest being measured. Also, one would like to minimize the current and charge magnitudes on instrumentation cables so that noise pick up is minimized. These and such other topological considerations are discussed in [4] from the results of earlier works [8, 9] and can be listed in summary format as follows.

a) The instrumentation cabling should become a part of or shielded by the conductor topology of the experiment.

b) If a local ground is available, the sensor-cable shield should stay in continuous electrical contact with it and not protrude in the region of measurement interest.

c) Any instrumentation packages should, if possible, be placed in a location where there is no scattering from them or, if there is scattering from packages, the sensor should be in a shadow region, with respect to such scattering.

d) Shields or conduits for cable routings should be used whenever possible to avoid direct coupling to cables.

The above considerations applied to the problem at hand, lead to locating the sensor at the end of a boom, which is long enough to minimize low frequency scattered field coupling. The sensor cable can then be routed through the boom. Furthermore, the fact that the free end of the boom is a current minimum or charge maximum for scattered quantities and is electrically connected to the aircraft strongly discourages an electric field measurement, by such an arrangement. For example, if the sensor is located at or near the free end of a nose boom, the boom could enter a radome and consequently it is desirable to run the sensor cables in a conduit while they traverse the length of the radome to the aircraft interior. An additional complication is introduced if the radar transmitting antenna is operating during the electromagnetic field measurement. This is a mutual effect where the hypothetical nose boom sensor and the radar in the nose of the aircraft can influence each other's performance, which should be minimized. Such are the complications and considerations arising out of sensor and conductor topology.

B. Symmetry Considerations

In the present application where the sensor is removed from the airframe, one can take advantage of the symmetry of the sensor, cabling, and EM field configuration. This is achieved by

a) cabling configured orthogonal to the incident electric field

and/or

b) fields scattered by the cable not being picked up by the sensor.

Alternatively, the cable scattering problem can also be removed by telemetring the data from the vicinity of the sensor. This is imperative for electric field measurement and optional for magnetic field measurement.

For the measurement of the antisymmetric part of the incident magnetic field, the symmetry considerations play a powerful and important role in designing sensor geometry. The sensor may be located at the end of a nose boom or a tail boom, and the cables routed through the interior of the boom.

For example, a four-gap magnetic-field sensor with its axis coincident with the boom axis exhibits C_4 symmetry [10] with respect to the boom and the vertical symmetry plane of the boom and sensor are coincident with aircraft's symmetry plane.

IV. Selection of Antisymmetric Measurement on the Symmetry Plane

The physical quantities for measurement are the symmetric and antisymmetric electric and magnetic fields, illustrated in Figure 2 with reference to a cartesian (x, y, z) coordinate system. The symmetry plane P is the x-y plane and $\vec{r}$ is a general position vector, while $\vec{r}_m$ is its mirror image in the symmetry plane P . The symmetric and antisymmetric electromagnetic fields, in general, have all three nonzero components as shown. However, on the symmetry plane P , the symmetric electric field has only x and y components and the symmetric magnetic field is z directed. On P , the antisymmetric magnetic field has only x and y components while the antisymmetric electric field is z directed. The orientations of fields off and on the symmetry plane P shown in Figure 2 also suggest the proper orientations of sensors intended for their measurement. For a more detailed discussion of the symmetry decomposition of fields and measurements with respect to a symmetry plane see [7].

If one considers now measurements of incident magnetic fields, one can consider choices of sensor locations such as listed in Table 1. Of the six (measured quantity-sensor location) configurations listed, three (indicated by arrows in Table 1) are examined in further detail and the EM considerations are listed in Table 2. Note that measurements off P always entail two sensors symmetrically positioned and oriented with respect to P , with the two signals added or subtracted (with identical delays) to give the desired signal representing the symmetric or antisymmetric part. As such this is not a measurement of the incident field at a single point, thereby distorting the transient waveform, a price one pays to minimize interference from airplane scattering. One could invoke special data-processing schemes to unfold the incident waveform (also obtaining some information concerning direction of incidence and polarization). Such data-processing schemes need detailed investigation.

If one instead constrains ones consideration to measurements on P the above difficulties vanish. One is measuring a single field component

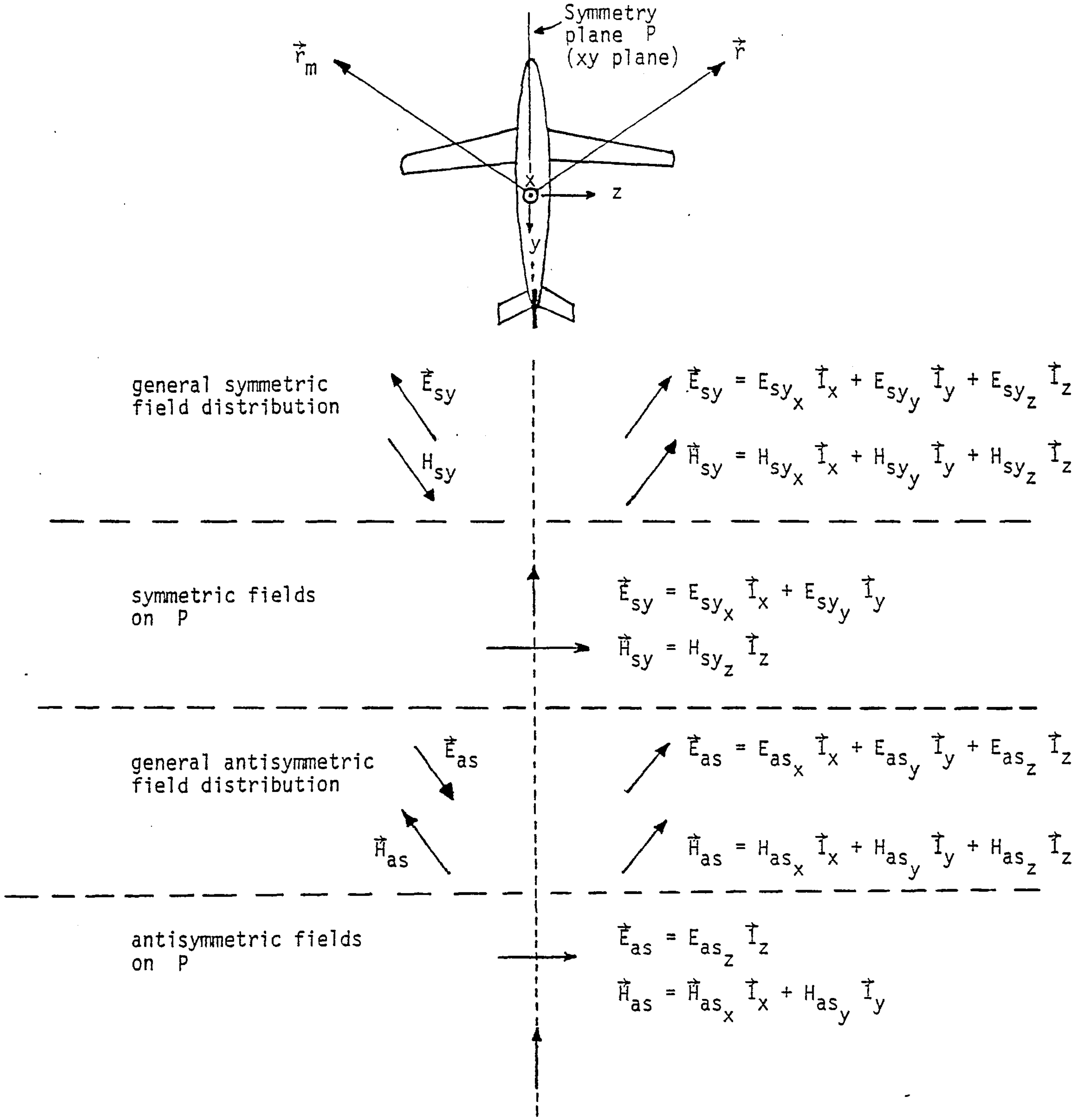

Figure 2. Symmetry plane, coordinate system, symmetric fields and antisymmetric fields.

Physical Quantity to be Measured	Preferred Locations and Orientations of Sensor(s)	
Symmetric part of $\vec{H}^{(inc)}$	2 sensors at wing tips	1
	1 sensor at the end of nose or tail boom with its axis perpendicular to P	
Antisymmetric part of $\vec{H}^{inc}$	2 sensors at wing tips	
	1 sensor at the end of nose or tail boom with its axis approximately parallel to fuselage	2
Antisymmetric part of $\vec{H}^{(inc)}$	2 sensors at wing tips	3
	1 sensor at the end of nose or tail boom with its axis approximately vertical	

TABLE 1. Magnetic field quantity to be measured along with preferred locations of sensors.

	Physical quantity to be measured	Possible Sensor geometry	Remarks
①	Symmetric part of incident $\vec{H}$	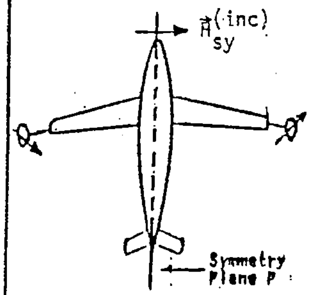	• Sum of outputs responds to incident symmetric $\vec{H}$ • Sum of sensor outputs insensitive to antisymmetric scattered $\vec{H}$ • Sensor axes not in general parallel • Sensors positioned off wing tip at minimum of symmetric wing scattering • Sensors tilted up and down to minimize symmetric fuselage scattering • Sensors rotated left and right to minimize symmetric vertical and horizontal stabilizer scattering
②	Anti-symmetric part of incident $\vec{H}$	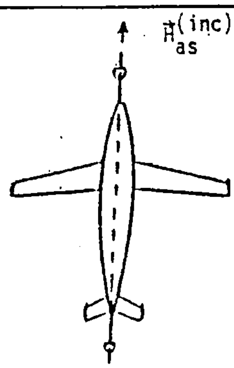	• Sensor in either location responds to incident antisymmetric $\vec{H}$ • Sensor is insensitive to symmetric scattered $\vec{H}$ (including main fuselage resonances) • Sensor responds to antisymmetric scattered field due to anti-symmetric wing and horizontal stabilizer currents which has to be minimized by position, orientation and physical distances.
③	Anti-symmetric part of incident $\vec{H}$	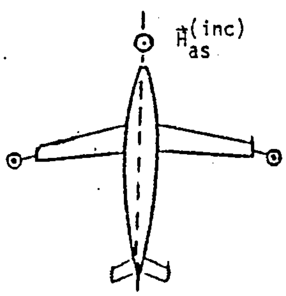	• Sum of sensor outputs responds to antisymmetric incident $\vec{H}$ • Sum of sensor outputs insentitive to symmetric scattered $\vec{H}$ • Sensor axes not in general parallel • Sensors positioned off wing tip at minimum of antisymmetric wing scattering • Sensors tilted left/right and fore/aft to minimize anti-symmetric scattering from wings and fuselage • Since this type of measurement is attempting to measure an approximately vertical $\vec{H}$, the horizontal stabilizer anti-symmetric scattering of necessity couples to the sum of sensor outputs, which can be minimized by distance and smallness of horizontal stabilizer.

TABLE 2. Summary of some possible magnetic field measurement configurations and their salient features.

at a single position which eliminates the need for two sensors. Furthermore, if one considers only the magnetic field on P the non-zero components are

$$\vec{H}_{sy}^{(inc)} = H_z \vec{1}_z \tag{1}$$

$$\vec{H}_{as}^{(inc)} = H_y \vec{1}_y + H_z \vec{1}_z \tag{2}$$

Of course this limits us to only a subset of all the possible measurements utilizing symmetry with respect to P .

Of the three possible measurement schemes of Table 2, measurement of an antisymmetric incident magnetic field approximately parallel to the fuselage, by using one sensor at the end of a nose or tail boom appears to be the simplest. This configuration is examined in full detail in the following sections. It is noted that for any measurement scheme, it is important to estimate and minimize the coupling of any aircraft scattered field to the sensor to achieve the highest possible accuracy in measurement.

V. Minimization of Antisymmetric Coupling from Wings and Stabilizers

The selected configuration for detailed investigation is the measurement of the antisymmetric part of the incident magnetic field, when it is in the symmetry plane of the aircraft and approximately parallel to the fuselage axis. This is best accomplished by a sensor at the end of a tail or nose boom as described below.

Consider a general location $P(x, y, 0)$ for the sensor intended to measure the antisymmetric incident magnetic field illustrated in Figure 3. At locations P_s, the sensor has to be oriented along the direction $\vec{1}_W$ to minimize wing scattering pickup and it has to be oriented along $\vec{1}_H$ to minimize horizontal stabilizer scattering. These are conflicting requirements and furthermore, neither orientation responds maximally to the incident field. Now consider moving the point P_x of Figure 3 to location P_1 or P_2 shown in Figure 4. Contrary to a popularly believed law about failures [11], the locations P_1 and P_2 not only render $\vec{1}_W$ and $\vec{1}_H$ colinear but they also align with the incident field, assuming that the wing, horizontal stabilizer and sensor axis are coplanar. However, in practice, the wing and horizontal stabilizer may not be in the same plane, as illustrated in Figures 5 and 6 in which case an optimal sensor location can be determined from geometrical calculations that may be validated by scale model experimentation. Typically the wing is also not entirely in a plane normal to the symmetry plane of the aircraft. Such physical features of the wing and horizontal stabilizer lead to an antisymmetric coupling during the measurement of an antisymmetric component of the incident magnetic field. The error introduced can approximately be estimated as follows.

Figure 7 shows the two possible sensor locations, viz., at the end of nose or tail boom for the measurement of an antisymmetric component of the incident magnetic field. The coupling of the low-frequency antisymmetric scattered fields from the wings and horizontal stabilizers should be reduced to acceptable levels in such a measurement. If the wings or horizontal stabilizers are modeled by a conducting post (see Figure 8), the ratio of scattered to incident magnetic field is available [12]. In the case of

Sensor location

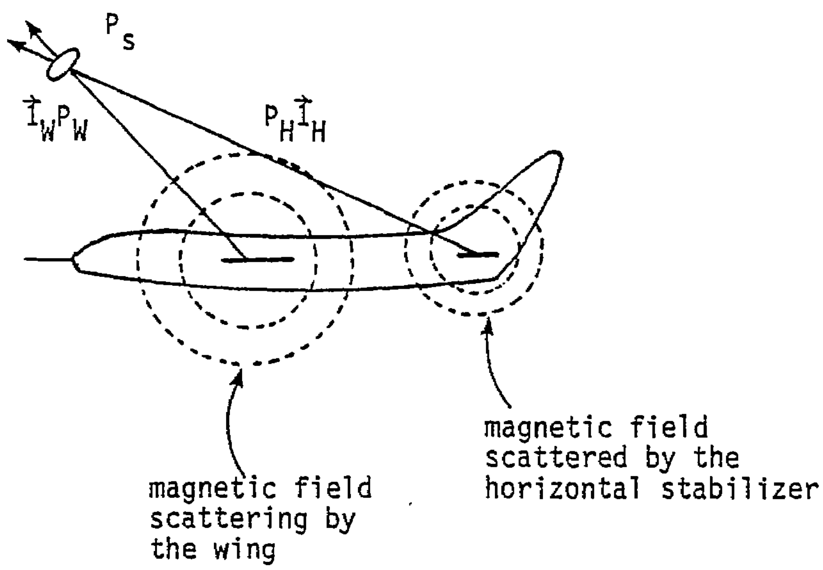

Figure 3. A general location and orientation for sensor where the wing scattering or the horizontal stabilizer scattering can be minimized, by orienting the sensor axis along P_W or P_H.

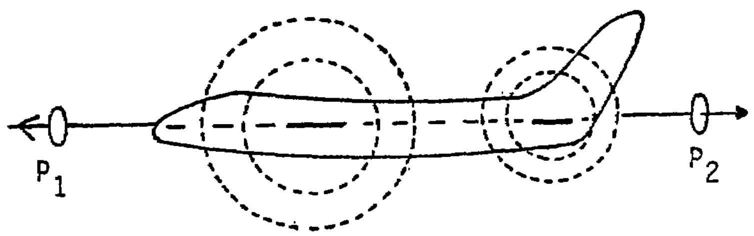

Figure 4. Sensor location and orientation which minimizes coupling from both wing and horizontal stabilizer (P_W and P_H coincide with each other and with the incident field quantity to be measured).

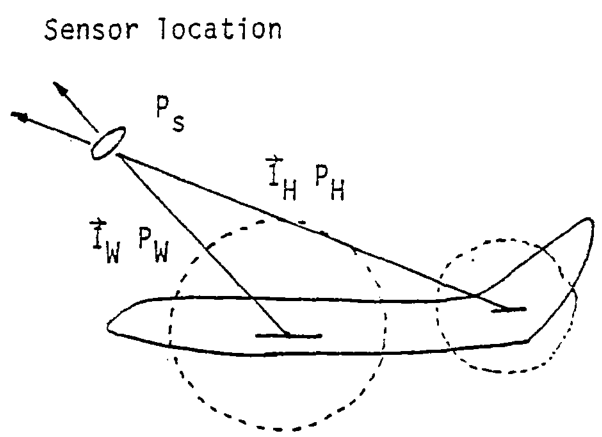

Figure 5. General sensor location for the case of wings and horizontal stabilizer in differenct planes.

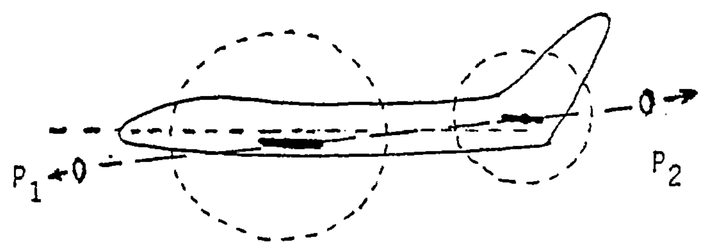

Figure 6. Location P_1 or P_2 such that coupling from both wing and horizontal stabilizer are determined from geometrical calculations and/or scale model experimentation.

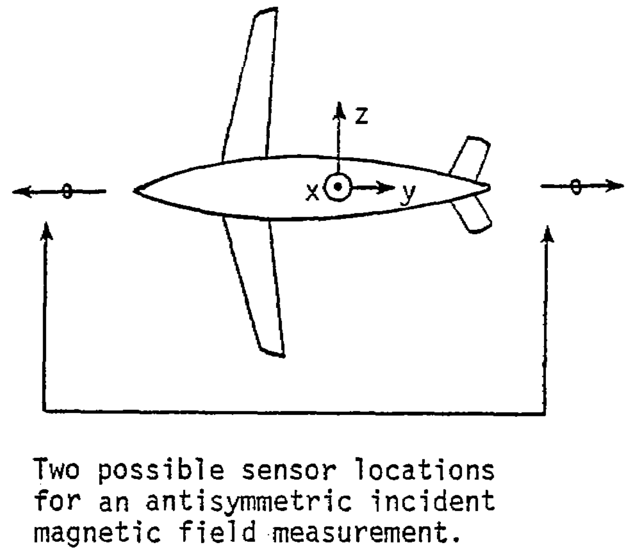

Figure 7. Measurement configuration for an antisymmetric component of the incident magnetic field.

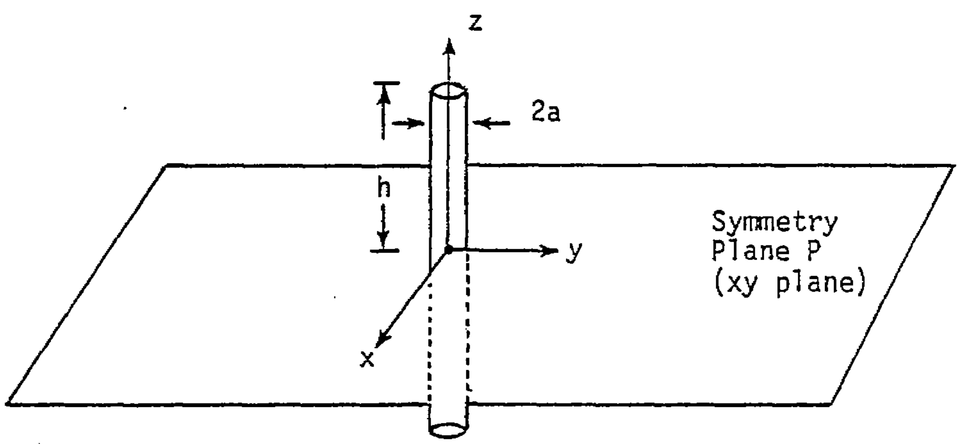

Figure 8. Conducting post model for the wing (or horizontal stabilizer).

aircraft with delta wings, it can be modeled by a rectangular plate which then can be modeled by [13] a conducting post of equivalent radius (a_{eq} = plate width/4). In Figure 5 of [12], the ratio of scattered to incident magnetic field is plotted as a function of ($\lambdabar/h$) for $a/h = 0.1$ for different values of R/h where

$\lambdabar$ ≡ radian wavelength = $\lambda/(2\pi)$

$2h$ ≡ total height of the conducting post

a ≡ radius of the conducting post

R ≡ distance of the observation point from the post.

The peak value for the ratio of scattered to incident field occurs for $(\lambdabar/h) = (0.7)$ or $(h/\lambda = 0.23)$ which corresponds to the case of a resonant post. Thus from the results of [12], it is noted that the maximum value of $[H^{(scat)}/H^{(inc)}]$ occurs when the post is resonant, i.e., $(h/\lambda \cong 0.23)$. Furthermore, the maximum value itself can be approximated by

$$\left|\frac{H^{(scat)}}{H^{(inc)}}\right| \cong \frac{h}{R} \qquad \text{for a resonant post} \tag{3}$$

However, because of the thickness and curvature of the wings (see Figure 9) or horizontal stabilizer, certain corrections to the above expression are in order. A simple and conservative estimate of this correction is (Δ/R) with Δ = the largest deviation of the wing from some plane (perpendicular to P and passing through the sensor) which minimizes Δ itself leading to

$$\left|\frac{H^{(scat)}}{H^{(inc)}}\right| \cong \frac{h}{R} \times \frac{\Delta}{R} \tag{4}$$

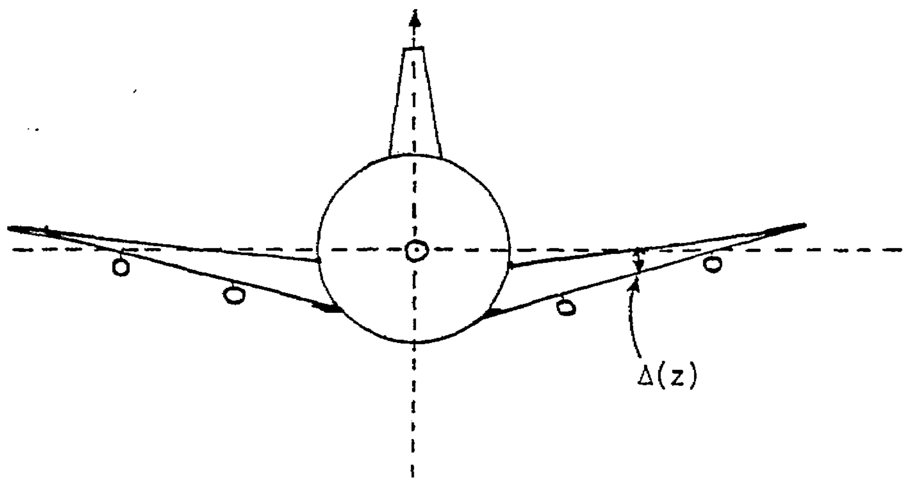

Figure 9a. Nose-on view of aircraft showing the wing and wing-engines thickness parameter Δ(z).

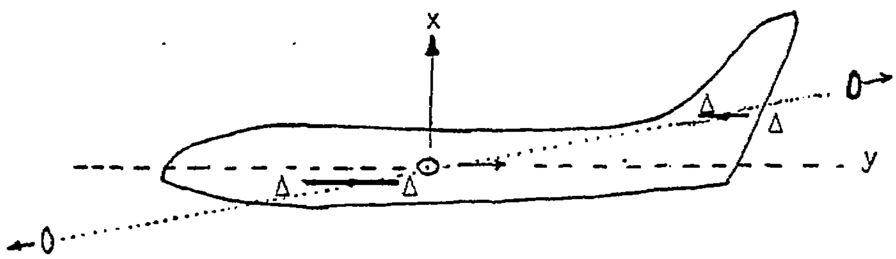

Figure 9b. Side view showing the angles "seen" by the sensor with respect to the wings and horizontal stabilizers. (Note that if the wing and horizontal stabilizer are not "coplanar" on a plane of constant x, then the sensor position is moved and orientation tilted to minimize sensitivity to combined wing and horizontal stabilizer scattering).

for the correction factor due to antisymmetric wing and horizontal-stabilizer coupling. Equation (4) can then be used in estimating an upper bound for the coupling from wings and horizontal stabilizers. The question of which of these two is predominant, is aircraft specific, depending on whether the nose or tail boom location is preferred.

VI. Quasimagnetostatic Antisymmetric Fields Scattered by Fuselage

In measuring the antisymmetric part of the incident magnetic field, the low frequency scattering from the cylindrical fuselage is a source of undesirable coupling, for both possible locations (aft or forward boom) of the magnetic field sensor. In view of this, it is desirable to estimate this error and locate the sensor sufficiently away from the airframe to reduce the effect to acceptable or tolerable levels.

Consider the geometry of the scatterer shown in Figure 10, as a model for the cylindrical fuselage. $H^{(inc)}$ is the antisymmetric part of the incident magnetic field to be measured, b is the radius of the sensing loop and a is the radius of the scattering model of the fuselage. The origin of coordinates is located at half a radius inside the tip of the fuselage. The scattered magnetic field due to a line of magnetic point dipoles of strength m is given by [14, 15]

$$\vec{H}^{(scat)}(\Psi, y) = -\frac{m}{4\pi}\nabla(1/r) = \vec{1}_\Psi H_\Psi + \vec{1}_y H_y \tag{5}$$

In component form, we have

$$H_\Psi = \frac{m}{4\pi}\frac{\Psi}{r^3} \quad \text{and} \quad H_y = \frac{m}{4\pi}\frac{y}{r^3} \tag{6}$$

Referring to Figure 10b, if Φ and $\Delta\Phi_o$ are the flux of the incident and scattered field respectively through the sensing loop, using $m = \pi a^2 H^{(inc)}$, we have

$$\begin{aligned} \frac{\text{Induced voltage (scat)}}{\text{Induced voltage (inc)}} &= \frac{\Delta\Phi}{\Phi} \\ &= \frac{\pi a^2 H_y^{(inc)}}{4\pi}\int_o^b d\Psi' \int_o^{2\pi} d\phi' \; \frac{y\Psi'}{r^3} \Big/ \left[\pi b^2 H_y^{(inc)}\right] \end{aligned} \tag{7}$$

and, for small loops ($b << y$) we have,

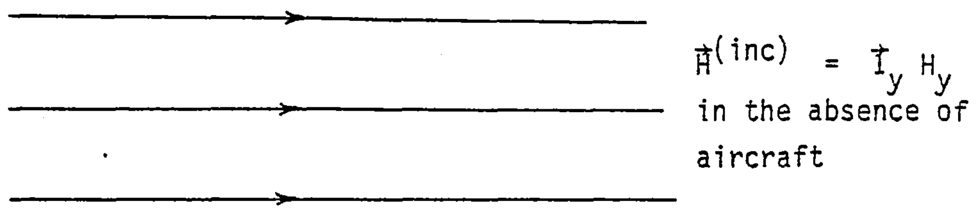

Figure 10(a). Incident magnetic field
(antisymmetric part)

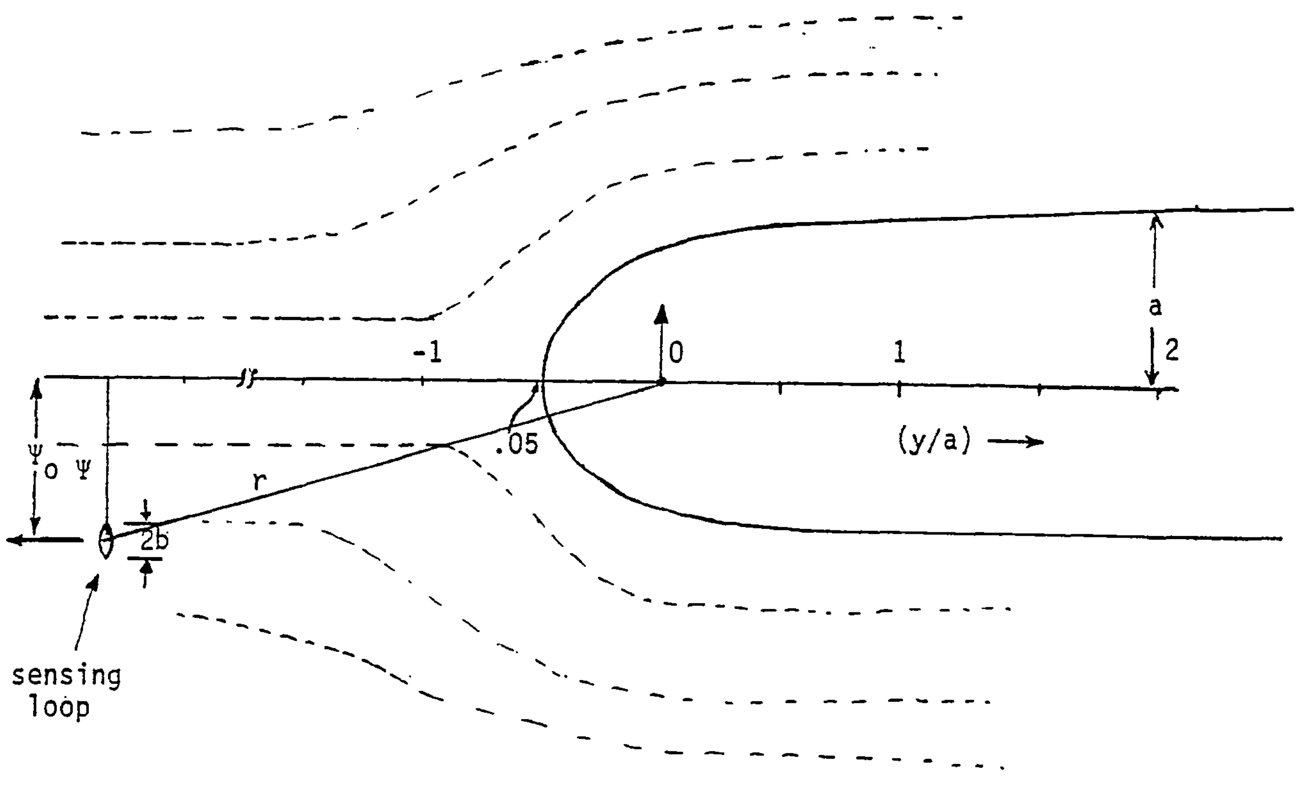

Figure 10(b). Scattering model for fuselage

$$\frac{\Delta\Phi}{\Phi} \cong \frac{H_y^{(scat)}}{H_y^{(inc)}} = -\frac{a^2}{4y^2}\left[1 + \left(\frac{\Psi_o}{y}\right)^2\right]^{-3/2} \tag{8}$$

where Ψ_o is the radial offset of the sensing loop. It is noted that the above expression reduces to

$$\frac{\Delta\Phi}{\Phi} \cong -\frac{a^2}{4y^2} \quad \text{for} \quad \Psi_o = 0 \quad \text{and when} \quad b \ll y \tag{9}$$

for the case of $\Psi_o = 0$ and is in agreement with the available expression in [14]. Also, when the sensing loop is off the axis, there is a radial component of scattered field given by equation (16), but the orientation of the sensing loop is such that, it is insensitive to the radial scattered field. In concluding this section, it is noted that equation (8) is useful in estimating the error introduced in measuring an antisymmetric incident magnetic field approximately parallel to the fuselage, due to quasi-static scattering from the fuselage.

VII. High-Frequency Antisymmetric Errors

Yet another source of error, while measuring the symmetric part of the incident magnetic field is the high-frequency scattered-field pickup. The high-frequency scattering can occur from surface features such as flat or curved surfaces (specular diffraction), edges, tips, and corners. For example, with reference to Figure 11, the bulkhead of the example aircraft is a source of high frequency scattering. In estimating the scattered fields, one may approximate the induced surface current by their "physical optics" values [16]. The physical optics values of surface currents can then be used in finding total and/or scattered fields. Using this procedure or other theories of diffractions, one can formally write down the scattered field [16] as

$$\vec{H}(\xi,s) \sim \vec{H}(0,s) \cdot \overleftrightarrow{C}(s)\, f_s(\xi)\, e^{-s\xi/c} \tag{10}$$

where

$\vec{H}(0,s)$ = incident field at 0

$f_s(\xi)$ = spread factor expressing the power conservation

$e^{-s\xi/c}$ = delay factor between 0 & P along the ray path

$\overleftrightarrow{C}(s)$ = dyadic diffraction coefficient depending on local geometry at the point of diffraction

ξ = distance between observation and diffraction points

Once again, referring to Figure 11, equation (10) can be approximated as

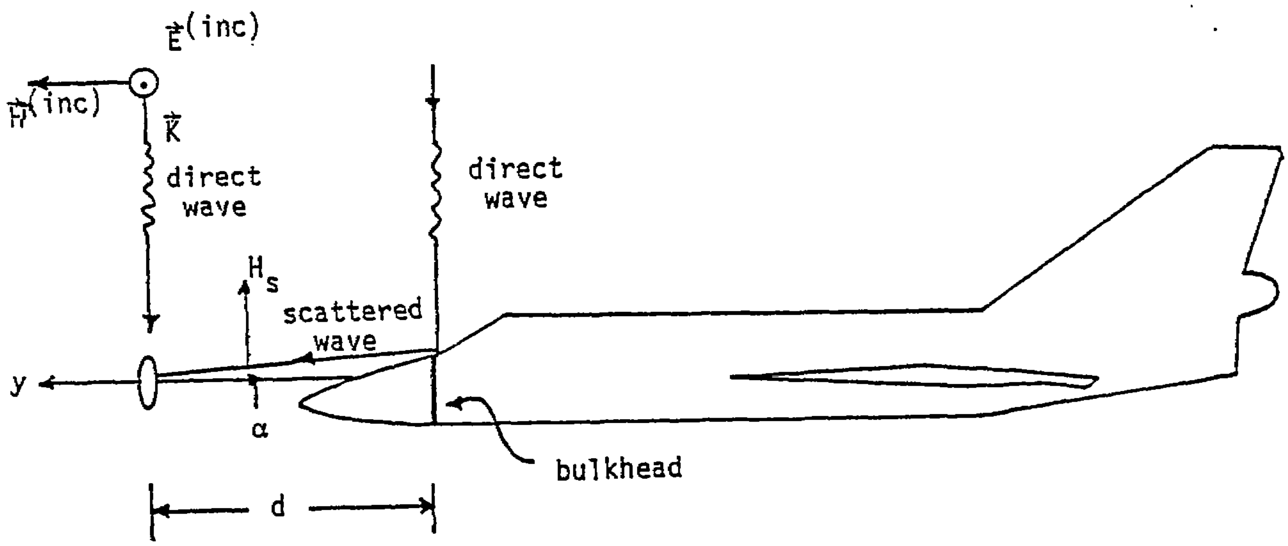

Figure 11. Example geometry for high-frequency scattering estimates.

$$\Delta_{hf} = \text{high-frequency error} = \left| \frac{H_y^{(scat)}}{H_y^{(inc)}} \right|$$

$$\cong \sin(\alpha) \times \text{diffraction coefficient} \times \text{spreading function} \quad (11)$$

Typical spreading function estimates for curved wedges, edges, cones, plane angular sectors are available [16], as exemplified by the following

$$f_s(\xi) = \rho_c/[\xi(\rho_c + \xi)] \quad \text{for curved wedge}$$

with ρ_c = distance between the diffraction point and the caustic on the diffracted ray (12)

$$f_s(\xi) = 1/\sqrt{\xi} \qquad \text{(edge)} \qquad (13)$$

$$f_s(\xi) = 1/\xi \qquad \text{(cones and plane angular sectors)} \qquad (14)$$

Equations (11) and (14), with diffraction coefficient approximated by unity can yield conservative error estimates. Such estimates are useful in designing the sensor location (i.e., picking a proper value of ξ that reduces the high frequency scattered field coupling to acceptable levels, during symmetric magnetic field measurement.

VIII. Forward or Aft Sensor Locations

The previous sections considered the measurement of the antisymmetric component of the incident magnetic field approximately parallel to the fuselage and led to the conclusion that an efficient way of performing this measurement is with a sensing loop at the end of a forward (nose) or aft (tail) boom. The choice of forward or aft is selected based on the detailed geometry of the aircraft. Several considerations come into play in this selection and the object of this note is to highlight some guidelines and necessary calculations required in making this choice.

Consider a typical fighter aircraft with one or two jet engines on the rear of the aircraft along the fuselage axis. The aft boom sensor, along the fuselage axis is thus ruled out indicating a possibility of a boom off of the vertical stabilizer. Once again, the sensor axis has to be optimized so that it is insensitive to antisymmetric wing scattering from wings and horizontal stabilizers, by properly tilting the sensor to look through the middle of these transverse elements. To determine the proper sensor orientation, one has to estimate the tilt angles for the beginning and end of wings. Yet another important consideration is the wind stream effects on a vertical-stabilizer boom. Consequently, for typical fighter aircraft with wings (e.g., delta) aft and engine(s) along the fuselage axis (see Figure 11) the choice of a nose boom is strongly suggested.

Figure 12 shows a few different types of aircraft geometries and a desirable location of sensor for the measurement of the antisymmetric component of the incident magnetic field approximately parallel to the fuselage. For example, Figure 12d shows an aircraft with a propeller in the nose making a nose boom rather difficult. In such a case, other locations such as aft boom and wing tip positions, should be examined in detail. In propeller driven aircraft, the effect of scattering from the propellers in various positions has to be estimated; it would seem desirable to have the sensors far from the propellers, to have the angles from the fuselage axis to the propellers as "seen" by the sensors small, and to have the sensors oriented to minimize coupling to the propeller scattering.

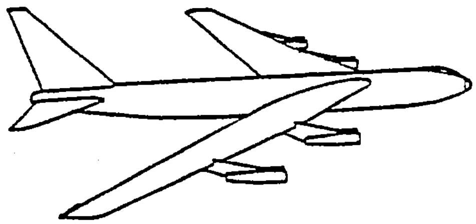

(a) Engines on the wings (aft and forward booms are possible, preferred location has to be determined by calculations or scaled experiments)

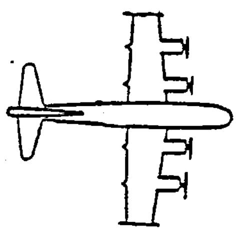

(b) Engines on the wings & wings forward (aft or tail boom)

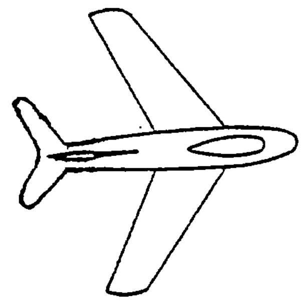

(c) Jet engine along fuselage axis (forward or nose boom)

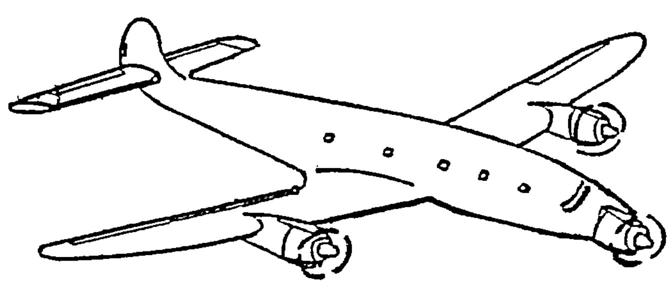

d) Propellers on the nose and wings (aft boom)

Figure 12. Typical aircraft geometries with a desirable sensor location in parenthesis for measurement of antisymmetric magnetic field approximately parallel to fuselage.

In summary, it is noted that the optimal sensor location is aircraft specific and it is possible that certain locations are impractical. For the possible locations, calculations of error estimates for the following undesirable coupling should be made, given an objective of measuring antisymmetric magnetic field, approximately parallel to the fuselage

(a) Antisymmetric coupling from wings/and horizontal stabilizers

(b) Antisymmetric field scattering from fuselage

(c) High-frequency antisymmetric errors

The above outlined calculations of error estimates should be performed for all possible sensor locations and the optimum location elected, based on error estimates and practical considerations.

IX. Summary

This note has made a beginning in the area of airborne platforms for the measurement of transient or broadband CW electromagnetic fields. This is electromagnetically a complex measurement given the requirement that an aircraft is used in the measurement, but its presence should not strongly influence the measured signals. The EM field (electric or magnetic) is arbitrarily oriented with respect to the aircraft, which makes it extremely useful to invoke symmetry considerations. Such considerations help in understanding both the incident and scattered fields in terms of non-interacting and complimentary components viz., symmetric and antisymmetric. Consequently, one can think of measuring the symmetric or antisymmetric part of the fields, one at a time. Also, it has been noted that the measurement of magnetic field is relatively easier than the electric field, from an operational or instrumentation point of view. Of the two components of the incident magnetic field, attention has been focused on the measurement of the antisymmetric part approximately parallel to the fuselage in this note. General considerations, guidelines for sensor locations, and ways of estimating possible errors in such a measurement have been discussed in detail. It is emphasized that optimal sensor location is highly aircraft specific, and suitable calculations of error estimates are mandatory before designing or fabrication of the sensor boom, mounts etc.

In concluding this note, it is observed that the subject area is vast and merits a lot of attention in future studies, e.g., measurement of other components of the magnetic field, electric field measurements, and associated error estimates.

References

1. C.E. Baum, E.L. Breen, F.L. Pitts, G.D. Sower and M.E. Thomas, "The Measurement of Lightning Environmental Parameters Related to Interaction with Electronic Systems," IEEE Trans. on Electromagnetic Compatibility, Vol. EMC-24, No. 2, pp. 123-137, May 1982. Also published as Sensor and Simulation Note 274, May 1982.

2. F.L. Pitts, "Electromagnetic Measurement of Lightning Strikes to Aircraft," AIAA Paper 81-0083, January 1981.

3. C.E. Baum, E. Breen, J.C. Giles, J. O'Neill and G.D. Sower, "Sensors for Electromagnetic Pulse Measurements Both Inside and Away from Nuclear Source Regions (Invited Paper)," IEEE Trans. on Electromagnetic Compatibility, Vol. EMC-20, pp. 22-34, February 1978. Also published as IEEE Trans. on Antennas and Propagation, Vol. AP-26, No. 1, pp. 22-35, January 1978, and as Sensor and Simulation Note 239, January, 1978.

4. C.E. Baum, "Sensors for Measurement of Intense Electromagnetic Pulses," Sensor and Simulation Note 271, June 1981, and in the Proceedings of the 3rd IEEE International Pulsed Power Conference, Albuquerque, NM, pp. 179-185, June 1981.

5. C.D. Taylor and T.T. Crow, "Calculation of Natural Resonances for Perpendicular Crossed Wires Parallel to an Imperfect Ground," Electromagnetics, Vol. 3, No. 1, pp. 41-64, January-March 1983.

6. C.D. Taylor, V. Naik and T. Crow, "A Study of the EMP Interaction with Aircarft Over an Imperfect Ground Plane," Interaction Note 362, May 1979.

7. C.E. Baum, "Interaction of Electromagnetic Fields with an Object which has an Electromagnetic Symmetry Plane," Interaction Note 63, 3 March 1971.

8. C.E. Baum, "The Role of Scattering in Electromagnetic Interference Problems," Electromagnetic Scattering, edited by P.L.E. Uslenghi, Academic Press, 1978.

9. Mini-Symposium on Electromagnetic Topology, FULMEN 4, University of New Mexico, March 1980.

10. M. Hammermesh, Group Theory and its Application to Physical Problems, Addison-Wesley, 1962.

11. Arthur Bloch, Murphy's Law and Other Reasons Why Things Go Wrong, Price, Stern, and Sloan Publishers, October 1977.

12. R.W. Sassman, R.W. Latham and A.G. Berger, "Electromagnetic Scattering from a Conducting Post", Sensor and Simulation Note 45, June 1967.

13. H. Jasik, Editor, Antenna Engineering Handbook, Chapter 3, "Characteristics of Linear Antenna Elements," by C.T. Tai, McGraw Hill, 1961.

14. R.W. Latham and K.S.H. Lee, "Magnetic Field Distortion by a Specific Antisymmetric, Semi-infinite, Perfectly Conducting Body", Sensor and Simulation Note 102, April 1970

15. J.C. Slater and N.H. Frank, Electromagnetism, McGraw Hill, New York, pp. 55, 1947

16. EMP Interaction: Principles, Techniques, and Reference Data (A Compleat Concatenation of Technology from the EMP Interaction Notes), EMP Interaction 2-1, Editor K.S.H. Lee, December 1980, AFWL-TR-80-402.